

Title: Effects of heat and freeze on isolated erythrocyte submembrane skeletons

Running title: Study on submembrane skeleton

Create date: 2016-09-21

<i>Name</i>	<i>Affiliations</i>
Professor Ivan Tanev Ivanov	1. Physics, biophysics, rentgenology and radiology, Medical Faculty, Thracian University, Stara Zagora, Bulgaria
Boyana Paarvanova	1. Physics, biophysics, rentgenology and radiology, Medical Faculty, Thracian University, Stara Zagora, Bulgaria
Professor Veselin Assenov Ivanov	1. Department of Chemistry and Biochemistry, Medical Faculty, Thracian University, Stara Zagora, Bulgaria
Kathrin Smuda	1. Institute of Transfusion Medicine, Charité-Universitätsmedizin , Berlin, Germany
Hans Bäumlner	1. Institute of Transfusion Medicine, Charité-Universitätsmedizin , Berlin, Germany
Assoc Professor Radostina Georgieva	1. Institute of Transfusion Medicine, Charité-Universitätsmedizin , Berlin, Germany

Corresponding author: Professor Ivan Tanev Ivanov <ivanov_it@gbg.bg>

Abstract

In this study we heated insoluble residues, obtained after Triton-X-100 (0.1 v/v %) extraction of erythrocyte ghost membranes (EGMs). Specific heat capacity, electric capacitance and resistance, and optical transmittance (280 nm) sustained sharp changes at 49°C (TA) and 66°C (TC), the known denaturation temperatures of spectrin and band 3, respectively. The change at TA was selectively inhibited by diamide (1 mM) and taurine mustard (1 mM) while its inducing temperature was selectively decreased by formamide in full concert with the assumed involvement of spectrin denaturation. In the residues of EGMs, pretreated with 4,4'-diiso-thiocyanato stilbene-2,2'-disulfonic acid (DIDS), the change at TC was shifted from 66 to 78°C which indicated the involvement of band 3 denaturation. The freeze and rapid thaw of EGM residues resulted in a strong reduction of cooperativity of band 3 denaturation while the slow thaw completely eliminated the peak of this denaturation. These effects of freeze-thaw were prevented in residues obtained from DIDS-treated EGMs. The freeze-thaw of residues slightly affected spectrin denaturation at 49°C although an additional denaturation appeared at 55°C. The results indicate preserved molecular structure and dynamics of the membrane skeleton in Triton-X-100 extracts of EGMs. The freeze-thaw inflicted strong damage on band 3 and spectrin-actin skeleton of EGM extracts which is relevant to cryobiology, cryosurgery and cryopreservation of cells.

Keywords: Triton-X-100 shells; spectrin; band 3; freeze-thaw; cryodamage.

Response to reviews:

response to reviews file - [download](#)

Supplementary files

Figure legends - [download](#)

1 Effects of heat and freeze on isolated erythrocyte submembrane skeletons

2
3 Ivan T. Ivanov⁽¹⁾, Boyana K. Paarvanova⁽¹⁾, Veselin Ivanov⁽²⁾, Kathrin Smuda⁽³⁾, Hans
4 Bäumler⁽³⁾, Radostina Georgieva^(1,3)

5
6 ⁽¹⁾ - Department of Physics and Biophysics, Medical Faculty of Thracian University,
7 Stara Zagora 6000, Bulgaria, E-mail: ivanov_it@gbg.bg

8 ⁽²⁾ - Department of Chemistry and Biochemistry, Medical Faculty, Thracian University,
9 Stara Zagora 6000, Bulgaria

10 ⁽³⁾ – Institute of Transfusion Medicine, Charité-Universitätsmedizin Berlin, 10117
11 Berlin, Germany

12
13
14
15
16
17
18
19
20 **Corresponding author:** Ivan T. Ivanov, Department of Physics and Biophysics,
21 Medical Faculty of Thracian University, Stara Zagora 6000, Bulgaria, E-mail:
22 ivanov_it@gbg.bg

24 **Abstract**

25 In this study we heated insoluble residues, obtained after Triton-X-100 (0.1 v/v %) extraction of erythrocyte ghost membranes (EGMs). Specific heat capacity, electric capacitance and resistance, and optical transmittance (280 nm) sustained sharp changes at 27 49°C (T_A) and 66°C (T_C), the known denaturation temperatures of spectrin and band 3, 28 respectively. The change at T_A was selectively inhibited by diamide (1 mM) and taurine 29 mustard (1 mM) while its inducing temperature was selectively decreased by formamide in 30 full concert with the assumed involvement of spectrin denaturation. In the residues of EGMs, 31 pretreated with 4,4'-diiso-thiocyanato stilbene-2,2'-disulfonic acid (DIDS), the change at T_C 32 was shifted from 66 to 78°C which indicated the involvement of band 3 denaturation. The 33 freeze and rapid thaw of EGM residues resulted in a strong reduction of cooperativity of band 34 3 denaturation while the slow thaw completely eliminated the peak of this denaturation. These 35 effects of freeze-thaw were prevented in residues obtained from DIDS-treated EGMs. The 36 freeze-thaw of residues slightly affected spectrin denaturation at 49°C although an additional 37 denaturation appeared at 55°C. The results indicate preserved molecular structure and 38 dynamics of the membrane skeleton in Triton-X-100 extracts of EGMs. The freeze-thaw 39 inflicted strong damage on band 3 and spectrin-actin skeleton of EGM extracts which is 40 relevant to cryobiology, cryosurgery and cryopreservation of cells.

42

43 *Key words:* Triton-X-100 shells, spectrin, band 3, freeze-thaw, cryodamage.

44

45 *Abbreviations:*

46 EGMs - erythrocyte ghost membranes, hypotonically isolated plasma membranes of

47 erythrocytes;

48 DSC – differential scanning microcalorimetry;

49 DIDS - 4,4'-diisothiocyanato stilbene-2,2'-disulfonic acid;

50 Triton-X-100 - polyethylene glycol p-(1,1,3,3-tetramethylbutyl)-phenyl ether;

51 Triton X-100 shells (residues) - under-membrane 2D-skeletons of EGMs, released as

52 insoluble residues after extraction of EGMs by Triton-X-100;

53 Diamide – diazenedicarboxylic acid bis(*N,N*-dimethylamide);

54 Taurine mustard (Taumustine) - 2-[bis(2-chloroethyl)amino]ethanesulfonic acid.

55

56 **1. Introduction**

57 The unique mechanical properties (deformability, elasticity and stability) of human
58 erythrocytes are mainly due to the erythrocyte plasma membrane and the association of its
59 membrane skeleton of peripheral proteins with its two major integral proteins, glycophorin
60 and band 3 (AE1, the anion exchanger) (Waugh and Agre, 1988; Low et al., 1991). The
61 membrane skeleton includes the third major protein of erythrocyte plasma membrane,
62 spectrin, and a set of minor proteins such as actin, ankyrin, band 4.1, band 4.2, ect (Mohandas
63 and Gallagher, 2008). While the deformability of erythrocyte plasma membrane depends
64 primarily on the state of spectrin-actin-glycophorin linkage, its mechanical stability chiefly
65 depends on the linkage of spectrin via ankyrin to the tetrameric forms of band 3 (Van Dort et
66 al., 1998; Alberts et al., 2008; Beutler et al., 2000) and on the interaction of spectrin with the
67 negatively charged lipids within the internal monolayer of lipid bilayer (Hendrich et al., 1991;
68 Michalak et al., 1994; Zwaal and Schroit, 1997). The remaining portion of band 3 is in
69 dimeric form and includes copies which freely diffuse within the lipid bilayer or are linked to
70 glycophorin (Reithmeier et al., 1996; Tanner, 1993).

71 Erythrocyte shape stability and transformation are subject to a complex mechanism
72 based on the minimum of the free energy of erythrocyte plasma membrane (Iglič, 1997;
73 Mukhopadhyay et al., 2002). The latter includes the elastic energy of membrane skeleton and
74 the bending energy of lipid bilayer as well as the free energy of embedded integral proteins
75 (Kralj-Iglič et al., 1996). This mechanism involves also the ratio of external to internal
76 monolayer area which could be affected by the conformation of major band 3 protein (**Gimsa**
77 **and Ried, 1995**). Results of Hianik et al. (2000) demonstrated that the role of the membrane
78 skeleton probably involves maintaining a higher compressibility of erythrocyte plasma
79 membranes.

80 The plasma membranes of many nonerythroid cells of mammals and birds also contain similar
81 anion exchanger protein (Alper, 1991) and submembraneous spectrin-actin network
82 (Mangeat, 1988). In humans, impairment of erythrocyte deformability and elasticity has been
83 correlated with many pathologic conditions, such as myocardial infarction, diabetes mellitus,
84 essential hypertension, hereditary spherocytosis, sickle cell anemia, and malaria (Simchon et
85 al., 1987; Chien, 1987; Mokken et al., 1992; Ajmani, 1997; Shelby et al., 2003; Delicou et al.,
86 2015).

87 Hypotonically isolated human erythrocyte ghost membranes (EGMs) have been extensively
88 studied with differential scanning calorimetry (DSC) which revealed several thermal
89 denaturations of specific EGM proteins. The denaturation of spectrin, as represented by the A
90 peak on the DSC thermogram, takes place at 49.5°C (Brandts et al., 1977). The cytoplasmic
91 domain of band 3 protein denatures at 62°C (B2 peak), and the membrane domain of the band
92 3 protein denatures at 67°C (C peak) (Snow, 1978).

93 A more simplified model of EGMs is frequently obtained by extracting EGMs with mild,
94 polar detergents, typically Triton-X-100. This procedure releases the erythrocyte plasma
95 membrane skeletons as insoluble residues, substantially delipidated and devoid of the most of
96 membrane integral proteins (Sharma and Gokhale, 2011). These, so called Triton-X-100
97 shells (residues) contain chiefly spectrin, actin and the portion of band 3 protein comprising
98 about 75 %, 5 % and 9 %, respectively, of their total residual protein (Lux et al., 1976). Other
99 proteins of the Triton-X-100 shells include ankyrin (about 3 %), band 4.1 (about 5 %), and
100 portions of band 4.2 (2 %). Triton X-shells preserve the shape and native two-dimensional
101 supramolecular assembly of the membrane skeleton of parent erythrocytes (Yu et al., 1973).
102 This is considered as evidence that membrane skeleton provides strong support for the shape
103 and mechanical stability of human erythrocytes.

104 Recent studies (Ivanov et al., 2012; Ivanov and Paarvanova, 2016) have noted changes in the
105 dielectric properties (complex impedance, Z^* , complex capacitance, C^* , dielectric loss curve)
106 of human erythrocytes and their isolated impermeable EGMs and Triton-X-100 shells,
107 induced at the spectrin denaturation temperature (49.5 °C). Based on the temperature
108 dependence of the loss curve, the spectrin skeleton of EGMs was considered dielectrically
109 active only at native state. Hence, the respective changes in Z^* and C^* at 49.5°C were
110 considered as contribution of spectrin skeleton to the dielectric properties of native EGMs.
111 Based on the strong frequency dependences of the changes in Z^* and C^* at 49.5°C, the
112 methods of dielectric spectroscopy (Klößgen et al., 2011) revealed two dielectric relaxations
113 on the membrane skeleton of EGMs. The first relaxation depended on the availability of
114 linkages between the integral proteins and spectrin and was detected at such frequencies
115 whereat the lipid bilayer did not allow penetration of the field into cytosole. It was present on
116 erythrocytes and impermeable EGMs and not on Triton-X-100 shells. It was explained as a
117 direct piezoeffect on the flexible spectrin filaments with a mechanical force originating from
118 the frequency-dependent charging of lipid bilayer. The second relaxation was detected at
119 higher frequencies allowing direct interaction of alternating field with the spectrin dipoles,
120 presumably those formed on the triple-helical repeat units of spectrin monomers.
121 The present study is aimed at the exploration of Triton-X-100 shells of EGMs with emphasis
122 on dielectric changes related to the thermal denaturations of their major proteins, spectrin and
123 band 3. These denaturations were detected by ultraviolet spectrophotometry and DSC.
124 Thermal dielectroscopy detected two major dielectric relaxations of above mentioned second
125 type, coupled to these denaturations. A study of these thermally-induced dielectric changes
126 showed that freeze-thaw of shells altered the band 3 and spectrin, and the alternation of the
127 former was more pronounced than that of the latter. The rapid thaw of frozen shells strongly
128 modified the band 3 denaturation while the slow thaw resulted in its complete elimination.

129 **2. Materials and methods**

130 *2.1. Materials.* DIDS (4,4'-diiso-thiocyanato stilbene-2,2'-disulfonic acid), MgCl₂, NaCl,
131 phosphate buffer, diamide (diazenedicarboxylic acid bis(*N,N*-dimethylamide)), taurine
132 mustard (2-[bis(2-chloroethyl)amino]ethanesulfonic acid), Triton-X-100 (polyethylene glycol
133 p-(1,1,3,3-tetramethylbutyl)-phenyl ether), EDTA (ethylenediaminetetraacetic acid) and
134 formamide were purchased from Sigma Chemicals Co, St. Louis, MO, USA.

135 *2.2. Isolation of erythrocytes.* Human blood samples were obtained from healthy donors
136 (donor centres at Stara Zagora, Bulgaria and Charité, Berlin, Germany). Erythrocytes were
137 isolated by centrifugation (500 x g, 5 min) and three times washed in excess volume of cold
138 150 mM NaCl saline prior usage.

139 *2.3. Thermal stabilization of band 3 with DIDS.* DIDS is a membrane impermeable
140 bifunctional covalent amino reagent, specifically binding and cross-linking band 3 monomer
141 (Cabantchik and Greger, 1992). Washed erythrocytes were suspended at hematocrit of 0.10 in
142 150 mM NaCl saline, containing 5 mM phosphate buffer, pH 7.8, and 50 μM DIDS at dark
143 and at room temperature for 15 min. The DIDS - treated cells were isolated, twice washed in
144 excess volume of cold 150 mM NaCl saline to remove non-reacted DIDS. Under these
145 conditions, more than 95 % of the DIDS resides on band 3 (Jennings and Passow, 1979)
146 resulting in strong thermal stabilisation of this protein and shifting of its denaturation
147 temperature from 67°C to 80°C (Snow et al., 1978).

148 *2.4. Isolation of EGMs* (Dodge et al., 1963). One volume of cold, dense suspension of washed
149 erythrocytes (intact or DIDS-treated), hematocrit 0.60, was rapidly and vigorously diluted in
150 15 volumes of 1°C-cold hypotonic solution, containing 4 mM MgCl₂ and 5 mM phosphate
151 buffer, pH 7.8 and left at 4°C for 5 min. The obtained leaky EGMs, used for Triton-X-100
152 extraction, were isolated by centrifugation (4000 x g, 12 min) and additionally washed in the
153 indicated hypotonic solution.

154 *2.5. Preparation of Triton-X-100 shells of erythrocyte ghost membranes* (Yu et al., 1973).
155 One ml of cold, leaky EGMs were vigorously mixed with equal volume of cold, washing
156 solution (10 mM NaCl saline, 4 mM of MgCl₂, 5 mM phosphate buffer, pH 7.8), that
157 contained 0.2 % (w/v) Triton-X-100. When specially indicated, the EGMs were extracted at
158 concentrations of Triton-X-100 higher than 0.1 %. The contact of membranes with detergent
159 immediately turned their opaque suspension into a transparent medium. As the Triton-X-100
160 itself is a chelator of Mg²⁺, higher concentration (4 mM) of these ions were used. Phosphate
161 buffer was preferred to Tris as Tris solubilises and disrupts the Triton-X-100 shells. The
162 extraction of EGMs lasted 30 min at 4 °C. The obtained solution of crude, insoluble residues
163 was diluted by 3 volumes of the indicated cold, washing medium and centrifuged (8000 x g,
164 12 min) to sediment the residues. The packed white paste of crude residues (about 0.2 ml) was
165 immediately studied or, prior to study, additionally washed one, two or three times in excess
166 volume of the washing medium. The term Triton X-100 shells (erythrocyte membrane
167 skeletons, spectrin-actin skeletons) further means three-step washed shells, if not specifically
168 indicated.

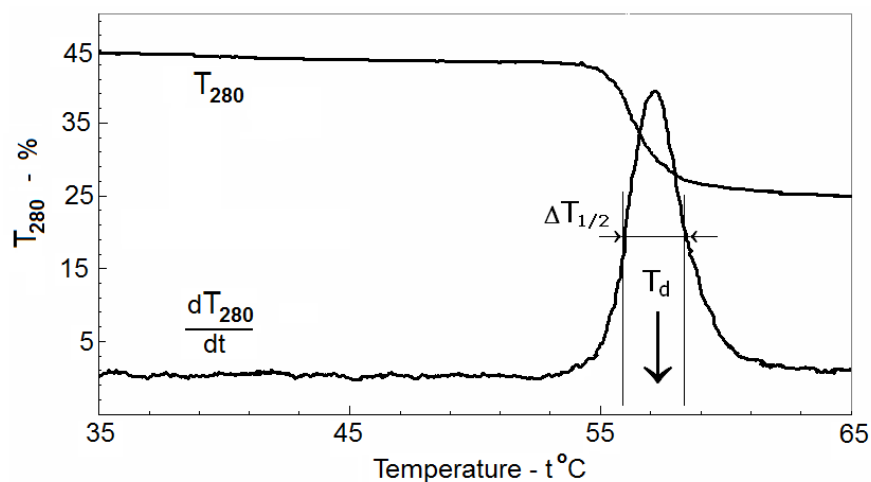
169 During the Triton-X-100 extraction of EGMs the residual protease activity could disrupt the
170 proteins of membrane skeletons, as shown by Ciana et al. (2005, 2011). This protease activity
171 originates from the white blood cell contamination of erythrocyte preparation. To reduce it at
172 the stage of erythrocyte isolation, the buffy coat containing the majority of white blood cells,
173 was carefully removed and the erythrocytes were thrice washed in excess volume of cold 150
174 mM NaCl saline. The usage of EGMs, isolated after the hypotonic lysis of erythrocytes,
175 additionally reduced protease activity.

176 *2.6. Differential scanning calorimetry of Triton-X-100 shells.* DSC measurements were
177 performed using the DSC unit of a MSC Microcalorimeter, MicroCal, MA, USA. The
178 measuring cell contained 1.442 ml Triton-X-100 shells, diluted in the washing medium at a

179 volume ratio of 1:0.3. The reference cell was filled with the washing medium. Scanning was
180 carried out with a heating rate of 0.7°C/min in the range from 20 to 90°C. Only two portions
181 of each sample were scanned if there was no substantial difference between the obtained
182 thermograms.

183 2.7. Spectrophotometric determination of thermal denaturations in Triton-X-100 shells

184 (Poklar et al., 1999). 2.6 ml of a solution containing 10 mM NaCl, 4 mM Mg²⁺ and 5 mM
185 phosphate buffer, pH 7.4, was placed in a quartz glass cuvette and the optical transmittance at
186 280 nm (T_{280}) was set at 100 %. Thereafter 40 µl of the Triton-X-100 shell paste was injected
187 in the solution reducing T_{280} to about 40 %. The optical transmittance was measured by a UV
188 spectrophotometer (Milton Roy Spectronic 21D, USA), equipped with an electric heater of
189 the measuring cuvette. Thermal denaturations were recorded heating the cuvette at a rate of
190 2°C/min. The temperature, t °C, of the solution was measured by an electronic thermometer
191 (accuracy 0.1°C). The analog output signals of the spectrophotometer and the thermometer
192 were both fed to a computer through a two-channel analog-to-digital converter.



193 *Fig. 1. Temperature profile of the optical transmittance at 280 nm, T_{280} (above), and of the*
194 *temperature derivative, dT_{280}/dt of T_{280} (below), of fibrinogen solution.*

195

196 The thermal denaturation of a test protein (fibrinogen) caused a sharp decrease in the optical
197 transmittance as a result of the unfolding of its polypeptide chain and the change (typically

198 decrease) in its molar volume. Spectrophotometric profile of the denaturation of fibrinogen
199 (0.03 wt. %), dissolved in 140 mM NaCl and 5 mM phosphate buffer, pH 7.4 is shown in Fig.
200 1. The obtained $T_{280} / t^{\circ}\text{C}$ profile demonstrated the denaturation as a sigmoid decrease with
201 midpoint at the temperature of denaturation, T_d . The derivative curve, dT_{280}/dt , in Fig. 1
202 corresponds to the rate of denaturation and specifies the top temperature of denaturation, T_d ,
203 and the half - width, $\Delta T_{1/2}$, of the denaturation peak.

204 2.8. *Thermal dielectroscopy of Triton X-100 shells* (Ivanov, 2010). The sample cuvette (a
205 cylindric glass tube with length = 120 mm, outer diameter = 4 mm and wall width = 0.5 mm)
206 contained two platinum wire electrodes mounted at a distance of about 4 mm from each other.
207 Prior to heating, 70 μl sample of the tested paste of Triton X-100 shells was placed in the
208 cuvette and deaerated at room temperature under vacuum for 5 min. The cuvette was put into
209 a hole, drilled into an aluminum block. The block was heated with constant heating rate.
210 During heating an alternating electric voltage of 80 mV was imposed between the electrodes
211 and the complex impedance, $Z^* = Z_{re} + jZ_{im}$, and complex capacitance, $C^* = C_{re} + jC_{im}$, of the
212 sample were continuously measured and separated into their real (Z_{re} and C_{re}) and imaginary
213 (Z_{im} and C_{im}) parts. Here, j is the imaginary unit, $j = (-1)^{0.5}$. Z^* and C^* were measured in a
214 sweep frequency mode at 12 frequencies between 0.05 and 10 MHz, scanned serially with
215 integration time of 0.5 s. The duration of each scan was less than 10 s. The core instrument
216 was a Solartron 1260 Impedance Analyzer (Schlumberger Instruments, Hampshire, England)
217 interfaced to Toshiba PC using the Miniscan software.

218 Platinum electrodes, low sample conductance (about 40 μS), low electrode voltage (80 mV)
219 and frequencies above 50 kHz were used in order to decrease electrode polarisation. The
220 Impedance Analyzer removes the noise and harmonic distortions and has 0.1% accuracy and
221 0.001 dB resolution.

222

223 **3. Results**

224 Micrographs, taken with confocal microscope, showed the crude Triton-X-100 shells as pale
225 mostly cup-shaped bodies with a diameter close to that of native erythrocytes (Fig. 2). Each
226 shell was covered with a number of small vesicles adhering to it. The maximum diameter of
227 these vesicles was 0.30 μm . Due to the low extracting concentration of the detergent, these
228 vesicles could contain residual amounts of EGM lipids and integral proteins, mostly band 3.

229

230

231

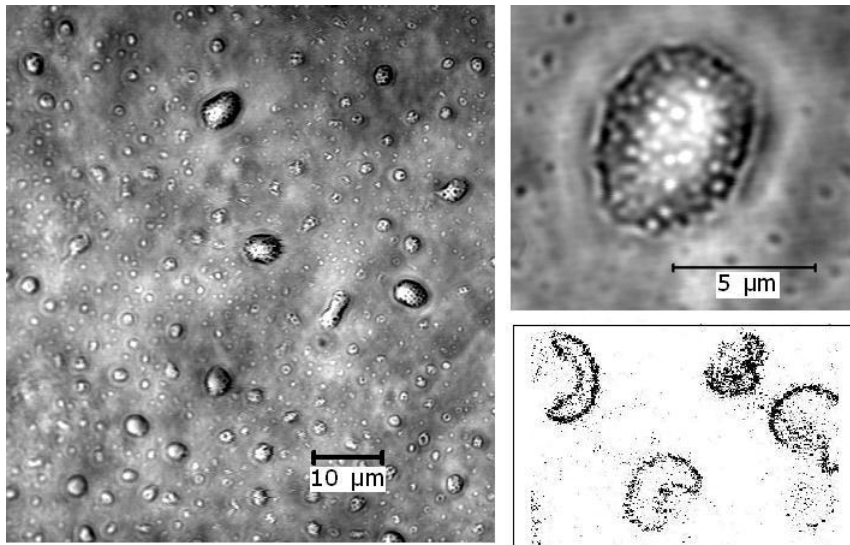
232

233

234

235

236



237 *Fig. 2. Micrographs of crude Triton-X-100 residues of EGMs. A general view (left) and*
238 *an image of single Triton-X-100 shell at higher magnification in transmission mode (top-*
239 *right). Confocal image of shells stained with the fluorescently labeled glycophorin-specific*
240 *antibody CD235a-PE in fluorescence mode (bottom-right). The images were taken with a*
241 *confocal laser scanning microscope (LSM 510, Zeiss, Jena, Germany).*

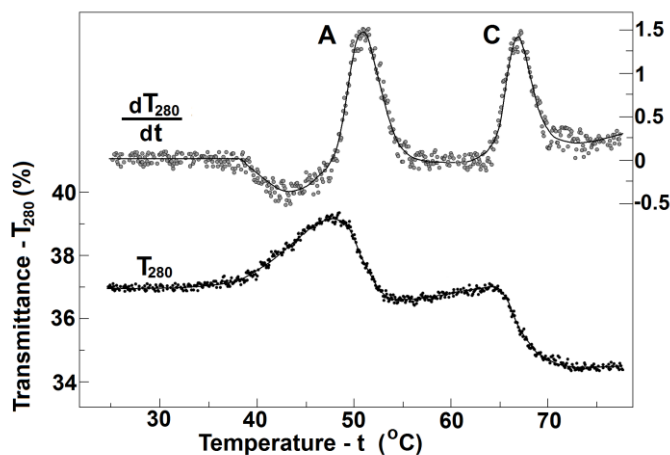
242

243 **3.1. Thermal denaturation of spectrin and band 3 of Triton-X-100 residues.**

244 Upon heating thrice washed Triton-X-100 shells the optical transmittance at 280 nm indicated
245 two sigmoid changes with transition mid-temperatures at T_A (49°C) and T_C (66°C) (Fig. 3,
246 lower curve). The temperature derivative of optical transmittance (Fig. 3, upper curve)
247 exhibited the indicated changes as narrow peaks (A and C), centred at the above mentioned

248 T_A and T_C temperatures. The narrow half-widths and high top temperatures of these peaks,
 249 compared to the denaturation peak of the test protein (Fig. 1), indicate involvement of protein
 250 denaturation in both events.

251 DSC scan of thrice washed Triton-X-100 shells exhibited two peaks of heat absorptions,
 252 centered at the same inducing temperatures, T_A (49°C) and T_C (66°C) (Fig. 4, curve 1). At the
 253 same inducing temperatures similar peaks have been calorimetrically obtained with samples
 254 of isolated EGMs and attributed to the heat denaturations of spectrin (the calorimetric A peak)
 255 and the integral domain of band 3 (the calorimetric C peak), respectively (Brandts et al., 1977;
 256 Ivanov et al., 2007). Hence, it could be assumed that the peaks at the T_A and T_C top
 257 temperatures on the spectrophotometric (Fig. 3) and DSC (Fig. 4) thermograms of Triton-X-
 258 100 shells corresponded to the heat denaturations of spectrin and band 3, respectively.



259
 260 *Fig. 3. Temperature profile of the optical transmittance at 280 nm, T_{280} (below), and the*
 261 *temperature derivative of T_{280} , dT_{280}/dt (above), of Triton-X-100 shells.*

262
 263 To additionally inspect these two denaturations, we subjected Triton-X-100 shell samples to
 264 continuous heating and measured the complex impedance and complex capacitance at various
 265 frequencies. At temperatures above 45°C, two irreversible sigmoid changes were registered
 266 on the temperature profiles (thermograms) of the real and imaginary parts of these parameters,

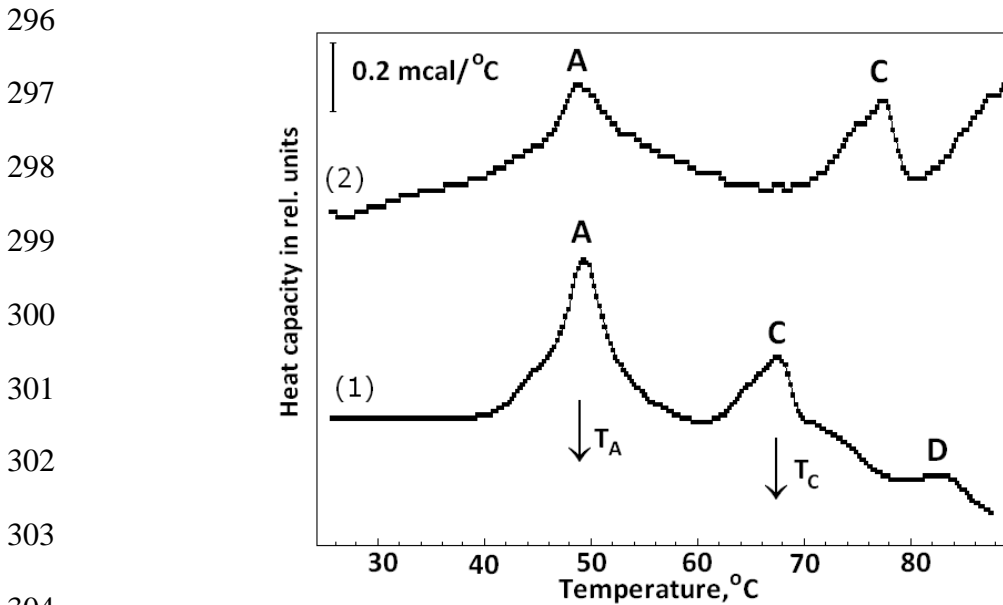
267 reflecting thermal damage to shells. For example, the changes on the thermogram of real
268 capacitance, C_{re} , measured at 1 MHz, are shown in Fig. 5. The amplitudes of the two changes,
269 ΔC_A and ΔC_C respectively, demonstrated remarkable frequency dependence (not shown). In
270 order better to determine the inducing temperatures of these changes the temperature
271 derivative of the sample capacitance (dC_{re}/dt) was also obtained (Fig. 5). The inducing
272 temperatures of these changes exactly coincided with above indicated denaturation
273 temperatures, T_A and T_C , respectively.

274 With once washed Triton-X-100 shells, the above indicated two sigmoid changes on the
275 capacitance and resistance thermograms were centred at lower temperatures, 46°C and 55°C,
276 respectively (not shown). Increasing the number of washings to three, the mid-temperatures of
277 these changes shifted upwards to the values, indicated in Fig. 5 and any additional wash did
278 not produced effect on these temperatures. This result indicates that the residual amounts of
279 Triton-X-100, remaining in the shells, reduced the above mentioned denaturation
280 temperatures. The complete removal of Triton-X-100 resulted in a less pronounced
281 temperature shift (3°C, from 46 to 49°C) of the first change and much more significant shift
282 (11°C, from 55 to 66°C) of the second change. Thus, the effect of Triton-X-100 on the
283 denaturation temperatures of spectrin and band 3 correlated the different ability of Triton-X-
284 100 to bind and destabilize the peripheral and integral proteins of EGM, respectively.

285 The membrane skeletons of EGMs were also obtained after extraction of leaky EGMs with
286 Triton-X-100 at the concentrations of detergent higher than 0.1 %. Typically 0.1 % (v/v)
287 Triton-X-100 is sufficient to lyse erythrocytes, and even up to 0.4 % concentrations will
288 usually not harm most enzymes which are isolated. The sediment of insoluble residues,
289 obtained at higher Triton-X-100 concentrations, had smaller volume. With increasing
290 concentration of detergent from 0.2 to 0.4 % the ΔC_A and ΔC_C amplitudes, as defined in Fig.
291 5, were reduced and at 0.8 % these amplitudes became undetectably small (not shown). This

292 result possibly indicates that EGM proteins became denatured by the detergent at the stage of
293 extraction due to the high detergent concentration.

294 3.2. *Effects produced on Triton X-shells by various reagents known for their specific impact*
295 *on erythrocyte plasma membrane proteins.*

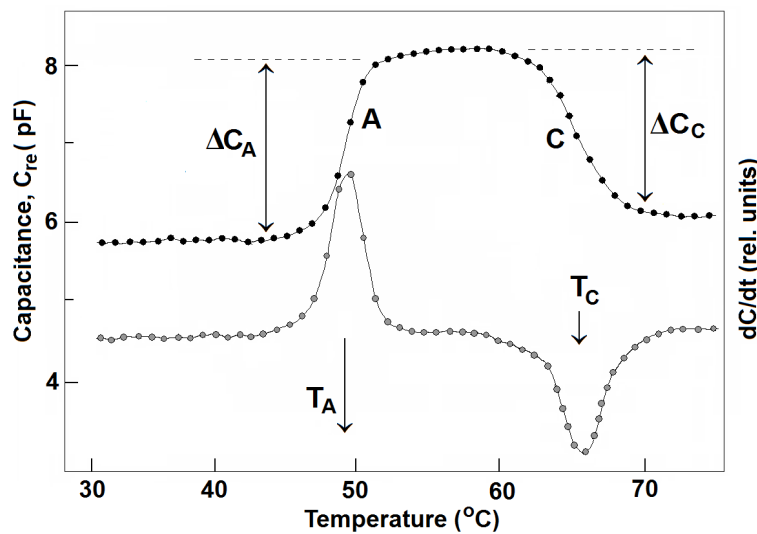


305 *Fig. 4. DSC thermograms of thrice washed Triton-X-100 shells of EGMs, isolated from*
306 *intact erythrocytes (1) and from DIDS-treated erythrocytes (2). The A, C and D-peaks*
307 *indicate the heat denaturation of spectrin, the anion exchanger and a peripheral protein*
308 *(probably tropomyosin). The suspension medium contained 4 mM MgCl₂ and 150 mM NaCl.*

309 *Protein content and the heating rate were 3 mg/ml and 0.7°C/min, respectively. The*
310 *membrane skeletons were released by extraction of EGMs with 0.25 % (v/v) Triton-X-100*

311
312 DIDS is a membrane-impermeable amino reagent, covalent inhibitor of band 3 of native
313 erythrocytes. At low (<50 μM) concentrations in outside medium it specifically binds band 3,
314 increasing its denaturation temperature step-wisely by 13°C (Snow et al., 1978). Using
315 Triton-X-100 shells, isolated from DIDS-treated erythrocytes, similar step-wise shift of T_C
316 from 66°C to 78°C was registered on their DSC thermogram (Fig. 4, curve 2) and on their

317 spectrophotometric, capacitance and resistance thermograms (not shown). At the same time,
 318 DIDS had no effect on the inducing temperature (T_A) of the first change. The same step-wise
 319 shift of T_C was obtained adding DIDS (final concentration 50 μ M) to Triton X-shells, isolated
 320 from intact EGMs, during the first wash of shells. In conclusion, this specific threshold effect
 321 of DIDS on thermal stability of Triton-X-100 shells, strongly supports the involvement of
 322 band 3 denaturation in the change at T_C .



323
 324 *Fig.5. Temperature dependence of the capacitance, C_{re} (●), and of the temperature*
 325 *derivative of the capacitance, dC_{re}/dt (o), of a sample of Triton-X-100 shells of EGMs. The*
 326 *detergent-insoluble skeletons were prepared by extraction of EGMs with 0.1 % (v/v) Triton-X-*
 327 *100. Amplitudes, ΔC_A and ΔC_C , of the capacitance changes due to the denaturations of*
 328 *spectrin and band 3 at the mid temperatures T_A and T_C , respectively, are shown. Arrows*
 329 *indicate the mid-temperatures of the sigmoid changes in sample capacitance. The washing*
 330 *medium contained 10 mM NaCl, 4 mM $MgCl_2$ and 5 mM phosphate buffer, pH 7.8. Protein*
 331 *content, heating rate and frequency were 30 mg ml⁻¹, 2.0°C/min and 1 MHz, correspondingly.*
 332

333 Diamide is a bivalent sulfhydryl reagent while taurine mustard is a dialkylating agent both
 334 specifically cross-linking spectrin dimers, when applied at low (1 mM) concentration on

335 native erythrocytes (Fischer et al., 1978; Wildenauer et al., 1980). While it is not bound itself,
336 diamide mediates the formation of disulfide bonds between spatially adjacent sulfhydryl
337 groups primarily in spectrin. Both inter- and intra-molecular disulfide bonds are formed:
338 about one per 30 spectrin dimers of the former type and one per three spectrin dimers of the
339 latter type. In this study, we exploited the specific action of diamide and taurine mustard
340 toward spectrin, adding these reagents to thrice washed Triton-X-100 shells at the final
341 concentration of 1 mM. Both reagents inhibited about 3-fold stronger the amplitude of the
342 sigmoid change at T_A compared to that at T_C (not shown), whereas the values of T_A and T_C
343 temperatures were not affected. This result is in line with the assumed involvement of spectrin
344 in the denaturation of Triton-X-100 shells at T_A . In addition, this result indicated that specific
345 cross-linking and resulting immobilisation of intramolecular segments of spectrin reduced the
346 dielectric polarisation of Triton-X-100 shells.

347 Polar organic solvents are heavily used in various biomedical applications. For example,
348 formamide lowers the melting temperatures of deoxyribonucleic acids linearly by 2.4 -
349 2.9°C/mole of formamide (Blake and Delcourt, 1996). This effect is used to accelerate the
350 hybridization of deoxyribonucleic acids. Applied on native erythrocytes and impermeable
351 EGMs, the great majority of polar organic solvents destabilised much stronger band 3 than
352 spectrin (Ivanov, 2001; Paarvanova et al., 2012). As an exception, formamide displayed a
353 specific ability to destabilise spectrin, decreasing its denaturation temperature at about 3 time
354 stronger rate compared to that of band 3. In this study, formamide demonstrated even more its
355 specific effect on the proteins of Triton-X-100 shells. At concentrations less than 7 % (v/v) it
356 reduced linearly the T_A and T_C . The former, however, was reduced at about a 10-fold higher
357 rate compared to the latter (not shown). This finding is in line with the assumed participation
358 of spectrin in the denaturation at T_A .

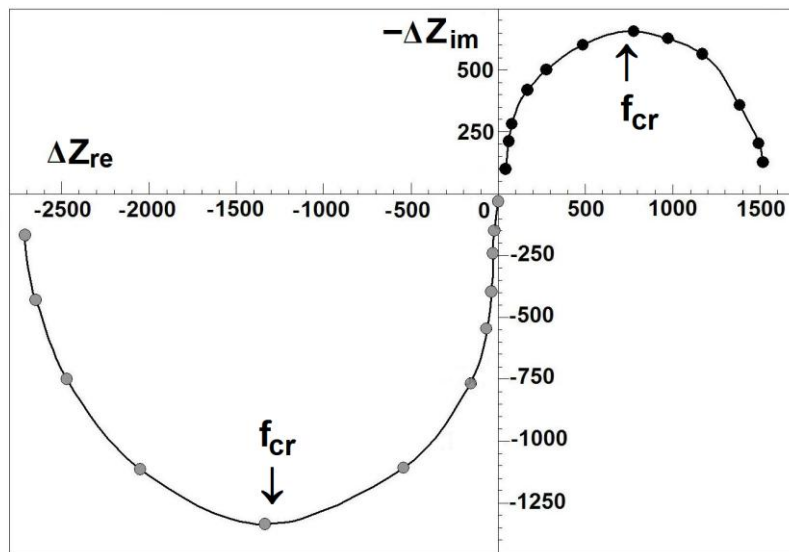
359 Added to the Triton-X-100 residues prior to heating, EDTA strongly reduced the amplitudes,
360 ΔC_A and ΔC_C , and decreased the inducing temperatures, T_A and T_C , on the capacitance and
361 resistance thermograms (not shown). For example, 5 mM EDTA inhibited about three times
362 the capacitance changes ΔC_A and ΔC_C (as defined in Fig. 3), and decreased the T_A and T_C by 4
363 °C and 11 °C, respectively. This result is in line with the known ability of EDTA to disrupt
364 the structure and solubilize the proteins of EGMs (McMillan and Luftig, 1973).

365 *3.3. Dielectric relaxations on spectrin and band 3 of Triton-X-100 residues.*

366 As noted above the amplitudes of detected changes at T_A and T_C on the complex impedance
367 and capacitance of Triton-X-100 residues displayed strong frequency dependences. These
368 frequency effects reflect the contribution of spectrin and band 3 to the dielectric polarisation
369 of Triton-X-100 residues as the amplitudes of both dielectric changes at T_A and T_C were
370 reduced to zero after the thermal denaturation of respective proteins. To inspect both
371 frequency dependences in more detail, dielectroscopy methods were further applied. They
372 allow get insight into the molecular mobility of electric dipoles associated to proteins
373 involved in respective dielectric relaxations. In contrast to the measurement of sample
374 impedance, the measurement of sample capacitance was impeded at frequencies, lower than
375 100 kHz due to the electrode polarisation. Thermograms of complex impedance, $Z^* = Z_{re} + j$
376 Z_{im} , were therefore used to investigate the frequency dependences of the amplitudes of the
377 dielectric changes at T_A and T_C .

378 The amplitudes of the detected change in Z_{re} at T_A were initially defined as $\Delta Z_{re} = (Z_{re})_{native} -$
379 $(Z_{re})_{denatured}$, where $(Z_{re})_{native}$ and $(Z_{re})_{denatured}$ are the real part of sample impedance at the native
380 state of spectrin (at a temperature 3°C less than T_A) and at the denatured state of spectrin (at a
381 temperature 3°C greater than T_A), respectively. This change, however, levels off within a
382 substantial temperature interval of about 6°C where it is superimposed on the continuous,
383 thermally induced change in the electrolyte conductivity. To compensate for the latter, which

384 had no relation to the temperature-induced event at T_A , the change in Z_{re} , taking place over an
 385 equal temperature interval prior the denaturation at T_A , was likewise determined and
 386 subtracted from the initial ΔZ_{re} . Using the same algorithm the amplitude of the real changes of
 387 Z_{im} at T_A , ΔZ_{im} , was determined and corrected for the thermally induced change in electrolyte
 388 conductivity. Also, the real corrected amplitudes of the changes in Z_{re} and Z_{im} at T_C were
 389 likewise determined and further used.

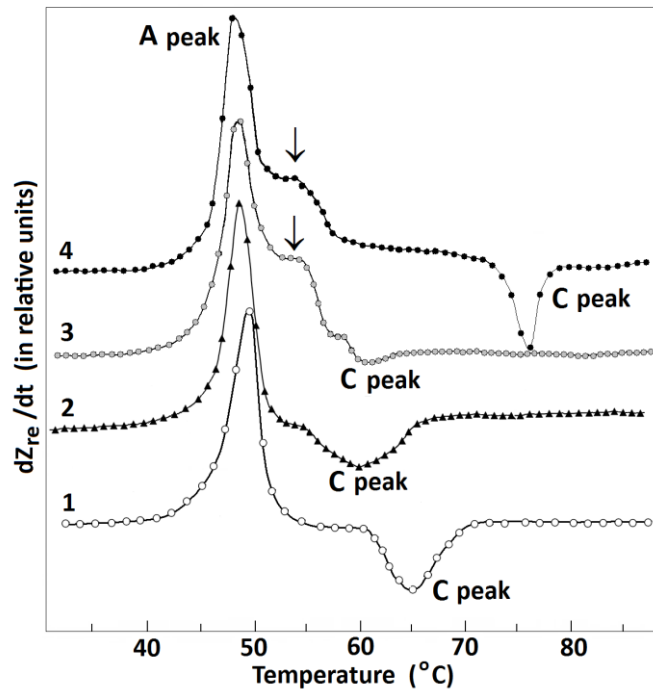


390
 391 *Fig. 6. Complex plane plot of $-\Delta Z_{im}$ vs ΔZ_{re} at the denaturation temperature of spectrin*
 392 *(o) and of band 3 (●). ΔZ_{re} and ΔZ_{im} are the amplitudes of the changes of the real and*
 393 *imaginary parts of complex impedance, respectively, of packed Triton-X-100 shells at the*
 394 *indicated temperatures of denaturation.*

395
 396 Based on the theory of dielectroscopy (Kell, 1987; Klösger et al., 2011) the frequency
 397 dependences of corrected amplitudes ΔZ_{re} and ΔZ_{im} were studied plotting the $-\Delta Z_{im}$ vs ΔZ_{re} for
 398 each denaturation temperature, T_A and T_C . Complex plane (Nyquist) plot of $-\Delta Z_{im}$ vs ΔZ_{re} ,
 399 determined at the spectrin denaturation temperature, T_A , had the form of a semicircle arc,
 400 situated below the argument axis (Fig. 6). The complex plane plot of $-\Delta Z_{im}$ vs ΔZ_{re} ,

401 determined at the band 3 denaturation temperature, T_C , represented another semicircle arc,
402 situated above the argument axis (Fig. 6). According to Kell (1987) and Klösgen et al. (2011)
403 each semicircle arc in Fig. 6 revealed a dielectric relaxation of Debye type, i.e. polarisation
404 mechanism with a single critical frequency, f_{cr} (a single relaxation time, $\tau = 1/(2\pi f_{cr})$).
405 As shown in Fig. 6, the $-\Delta Z_{im}$ vs ΔZ_{re} plot at the spectrin denaturation temperature revealed
406 only one dielectric relaxation due to the direct interaction of electric field with the dipole
407 moments of spectrin (Ivanov et al., 2012; Ivanov and Paarvanova, 2016). This finding is
408 consistent with the basic conception that Triton-X-100 residues lacked closed lipid bilayer
409 encapsulating them. The critical frequency, f_{cr} , for this relaxation is implicitly determined by
410 the top point of the corresponding semicircle arc, indicated by arrow in Fig. 6. From multiple
411 experiments ($n = 5$) with shells, isolated and washed at 10 mM NaCl concentration this
412 critical frequency was determined at 830 kHz (Fig. 6). With shells, isolated at 10 mM NaCl
413 and washed by media with increased NaCl concentration up to 120 mM the critical frequency
414 of spectrin relaxation linearly increased from 830 kHz to 9 MHz (not shown). The presence of
415 glycerol, known for its ability to strongly increase the viscosity of solutions, linearly
416 decreased the critical frequency of spectrin relaxation. For example, at 120 mM NaCl, this
417 critical frequency was decreased from 9 MHz at zero % glycerol to about 5 MHz at 40 %
418 glycerol (not shown). These data are in full concert with the same dependences, recently
419 reported for the spectrin skeleton of intact erythrocytes and impermeable EGMs (Ivanov and
420 Paarvanova, 2016) and indicate preserved molecular structure and dynamics of membrane
421 skeleton in Triton-X-100 shells.

422 On the other hand the critical frequency, f_{cr} , for the $-\Delta Z_{im}$ vs ΔZ_{re} plot at the denaturation
423 temperature of band 3 was determined 1300 kHz ($n = 5$). It did not depend on the NaCl
424 concentration (10 – 100 mM) and on the presence of glycerol (not shown). Both critical
425 frequencies were not affected by the preliminary DIDS-treatment of erythrocytes.



427

428 *Figure 7. Effect of freeze-thaw on Triton-X-100 residues as revealed by thermal*
 429 *dielectroscopy. The dZ_{re}/dt is the temperature derivative of the resistance, Z_{re} , measured at*
 430 *100 kHz, of Triton-X-100 residues. Residues were prepared from EGMs of intact erythrocytes*
 431 *(curves 1, 2 and 3) and from EGMs of DIDS-treated erythrocytes (curve 4). The control*
 432 *residues (curve 1) were not frozen, while the frozen residues were subjected to rapid thaw*
 433 *(curve 2) and slow thaw (curves 3 and 4).*

434

435 Thermal dielectroscopy was employed to investigate the alterations of major proteins, spectrin
 436 and band 3, induced by preliminary freeze-thaw of Triton-X-100 shells. In Fig. 7 these
 437 alterations are demonstrated by the temperature derivative of the resistance, Z_{re} , measured at
 438 100 kHz. A similar result was obtained using derivative thermograms of other components
 439 (Z_{im} , C_{re} and C_{im}) of complex impedance, Z^* , and capacitance, C^* , measured at various
 440 frequencies between 100 kHz and 5 MHz (not shown). The above mentioned dielectric

441 changes at T_A and T_C were altered in the residues subjected to preliminary freeze-thaw (Fig. 7,
442 curves 2, 3 and 4), compared to control shells not subjected to subzero temperatures (Fig. 7,
443 the curve 1). In addition, the frequency dependences of the amplitudes of respective dielectric
444 changes at T_A and T_C were used to determine the effect of freeze-thaw on respective dielectric
445 relaxations.

446 The effects produced by freeze-thaw on residues did not depend significantly on the value of
447 freezing temperature (-6, -16 and -80°C) and on the duration of freezing (1 to 10 h) however,
448 they strongly depended on the rate of thaw. When the frozen residues were rapidly thawed in
449 a water bath at 20°C for 10 min the denaturation C peak reduced its height, broadened its half-
450 width and preserved its area (Fig. 7, curve 2 compared to curve 1). This outcome indicated
451 preserved number of native protein copies and reduced cooperativity of their denaturation.

452 After slow thaw (4°C for 2 h) the predominant portion of the area of C peak was lost (Fig. 7,
453 curve 3 compared to curve 2) indicating strongly reduced number of native copies of band 3
454 in shells. The latter conclusion was confirmed by UV-spectrophotometry which detected that
455 the amplitude of C peak of frozen residues was three- to four-fold reduced after slow thaw
456 compared to rapid thaw (not shown).

457 The damage produced by the freeze and slow thaw on the band 3 was partially prevented by
458 the preliminary binding of DIDS to this protein. Compared to Triton-X-100 residues, obtained
459 from intact EGMs and not subjected to subzero temperatures (Fig. 7, curve 1), the
460 cooperativity and total area of the C peak were fully preserved in residues, obtained from
461 DIDS-treated EGMs and subjected to freeze and slow thaw (Fig. 7, curve 4). In addition, the
462 denaturation temperature, T_C , of band 3 of latter residues was increased by 13°C (Fig. 7, curve
463 4), a shift characteristic to DIDS-treated EGMs (Snow et al., 1978). However, the protective
464 effect of DIDS was partial as the relaxation frequency of band 3 in DIDS-treated residues was
465 decreased from 1300 kHz in residues not subjected to freeze-thaw to 350 kHz in residues

466 subjected to freeze-thaw (not shown). This outcome possibly indicates that freeze-thaw
467 produced aggregation and clustering of band 3.
468 Compared to band 3, spectrin was mildly damaged by the freeze-thaw of Triton-X-100
469 residues. The freeze-thaw cycle did not affect the cooperativity of spectrin denaturation as
470 expressed by the preserved height and half-width of the A peak. The inducing temperature,
471 T_A , of this peak was, however, slightly decreased (Fig. 7, curves 2 and 3 compared to curve
472 1). The relaxation frequency of dipoles associated to spectrin, 830 kHz at 10 mM NaCl,
473 preserved its value after freeze and slow thaw of Triton-X-100 residues. This result also
474 underlined the low cryosensitivity of spectrin, compared to that of band 3.
475 In contrast to the rapid thaw (Fig. 7, curve 2), the slow thaw of residues produced a shoulder
476 of the A peak centered at a temperature 6°C above T_A (Fig. 7, indicated by arrow on the
477 curves 3 and 4). The new denaturation was not affected by the preliminary stabilisation of
478 band 3 with DIDS (Fig. 7, curve 4). The relaxation frequency of the protein involved was very
479 low, about 200 kHz, possibly indicating the involvement of aggregated and clustered copies.
480 This protein could be peripheral one, similar to spectrin, but its identity is not known at
481 present.

482 4. Discussion

483 This study tested the structural stability of major proteins, spectrin and band 3, of Triton-X-
484 100 shells of EGMs as represented by the temperature and cooperativity of their thermal
485 denaturations. During the denaturations of spectrin at 49.5°C (T_A) and band 3 at 66°C (T_C) the
486 capacitance, C_{re} , and resistance, Z_{re} , of the sample of Triton-X-100 shells both changed in the
487 same direction, increasing at T_A and decreasing at T_C for any frequency within the 50 kHz -
488 10 MHz interval. The changes in resistance appear consequent upon the changes in
489 capacitance (dielectric polarisability) of Triton-X-100 shells and related changes in the
490 resultant electric field. This conclusion is consistent with the above mentioned basic

491 conception that each Triton-X-100 shell represented a network of proteins devoid of closed
492 lipid bilayer surrounding them and, in contrast to intact erythrocytes and their resealed EGMs
493 (Ivanov and Paarvanova, 2016) it was fully transparent to the incident electric field with any
494 frequency from the indicated frequency interval.

495 As shown in Fig. 2, a great number of tiny spheres (sphere-shaped vesicles) were firmly
496 attached to the spectrin skeleton of Triton-X-100 shells. These objects could be envisaged as
497 liposomes (closed **inside-out** lipid bilayers) made up of the remainder of original lipid bilayers
498 and band 3 copies of EGMs. We assume the attachment spots could include band 3 tetramers
499 which avoided the solubilisation, preserved a portion of their original lipid milieu and
500 remained strongly linked to spectrin via the ankyrin bridges of EGMs. This assumption is
501 consistent to the result (Fig. 5) that within the entire frequency interval of 50 kHz - 10 MHz
502 the capacitance (dielectric polarizability) of Triton-X-100 shells decreased at T_C indicating
503 immobilization of dielectrically active segments of band 3 copies after the denaturation of
504 band 3. This decrease in polarizability could be explained with the restriction imposed by the
505 lipid bilayer of attached liposomes on the mobility of band 3 dielectrically active segments
506 after band 3 denaturation at T_C .

507 By contrast, within the entire frequency interval of 50 kHz - 10 MHz the capacitance
508 (dielectric polarizability) of Triton-X-100 shells increased at T_A (Fig. 5) indicating that
509 dielectrically active segments of spectrin increased their mobility after the spectrin
510 denaturation. Previous study (Ivanov and Paarvanova, 2016) reported that the change of the
511 capacitance (dielectric polarizability) of intact erythrocytes and impermeable EGMs at the
512 spectrin denaturation temperature (49.5°C) depended on frequency; it decreased at low
513 frequencies (50 kHz - 3 MHz) and increased at higher frequencies (3 – 10 MHz). This
514 frequency effect was explained by the adherence of a part of denatured spectrin to the
515 encapsulating lipid bilayer resulting in partial immobilization of dielectrically active spectrin

516 segments and hardening of erythrocyte plasma membrane. Combining the above two lines of
517 evidence we arrive again at the basic conception that Triton-X-100 shells lacked an
518 encapsulating lipid bilayer thus the dielectrically active segments of spectrin were free to
519 demonstrate higher mobility in the denatured than in native state of spectrin.

520 Fig. 7 shows a damage of the band 3 protein as well as the spectrin-actin membrane skeleton
521 after freezing and thawing the Triton-X-100 residues. The freeze-thaw of residues had minor
522 effect on spectrin denaturation at 49°C although an additional protein denaturation appeared
523 at 55°C. The freeze and rapid thaw of Triton-X-100 residues resulted in a strong reduction of
524 cooperativity of band 3 denaturation while the slow thaw completely eliminated the peak of
525 this denaturation. The latter outcome is indicative of a substantial denaturation and/or
526 detachment of band 3 copies of the residues. These effects of freeze-thaw were prevented in
527 residues obtained from DIDS-treated EGMs supporting the view that the main damage
528 implicated the membrane protein band 3. Additional study is needed to elucidate the possible
529 damage induced by freeze /thaw on the band 3 linkage to membrane skeleton. In general,
530 these finding are in line with other reports (Woelders and Malva, 1998) that slow thaw is
531 particularly damaging to cells during their recovery after cryopreservation. The above results
532 could help design new experiments for finding optimal conditions to reduce the freeze
533 damage to erythrocytes and other cells. Based on the similarity of the general structure of
534 plasma membrane in erythrocytes and nucleated animal cells these results could be helpful for
535 cryobiology, cryosurgery and the cryopreservation of cells and tissues.

536 Compared to deoxyribonucleic acids the sensitivity of spectrin denaturation temperature to
537 formamide was several times higher (Ivanov, 2001; Paarvanova et al., 2012). This outcome
538 could be exploited for the design of drugs, which could be targeted to the major peripheral
539 proteins, homologous to erythrocyte spectrin, in human and animal cells.

540

541
542
543
544
545
546
547
548
549
550
551
552

4. Conclusions

Heat and the freeze greatly affected the structural stability and dielectric properties of erythrocyte membrane skeletons, released after mild extraction of erythrocyte ghost membranes by Triton-X-100. The thermal methods applied well differentiated the thermal (structural) stability of spectrin and band 3, and the contributions of these major proteins to the dielectric properties of Triton-X-100 shells. The results presented indicate that Triton-X-100 shells preserved the native structure of spectrin and band 3. The Triton-X-100 shells appear as a helpful model for exploration on the structure and dynamics of erythrocyte plasma membrane proteins and their change under a variety of adverse conditions, especially during freeze and slow/rapid thaw.

REFERENCES

- 553
- 554
- 555 Ajmani R. S. (1997): Hypertension and hemorheology. *Clin. Hemorheol. Microcirc.*
- 556 *17, 397-420*
- 557 Alberts B., Johnson A., Lewis J., Roberts K., Walter P., Baff M. (2008): *Molecular*
- 558 *Biology OfThe Cell. 5th Ed. Garland Science Publishing. New York*
- 559 Alper S. L. (1991): The band 3-related anion exchanger (AE) gene family. *Annu. Rev.*
- 560 *Physiol. 53, 549-564*
- 561 Beutler E., Lichtman M. A., Coller B. S., Kipps T. J., Seligshon U. (2000): *Williams*
- 562 *Hematology. 6th Ed. McGraw-Hill Professional. New York*
- 563 Blake R. D., Delcourt S. G. (1996): Thermodynamic effects of formamide on DNA
- 564 *stability. Nucleic Acids Res. 24(11), 2095-2103*
- 565 Brandts J. F., Erickson L., Lysko K., Schwartz A. T., Taverna R. D. (1977):
- 566 *Calorimetric studies of the structural transitions of the human erythrocyte membrane. The*
- 567 *involvement of spectrin in the A transition. Biochemistry. 16, 3450-3454*
- 568 Brandts J. F., Erickson L., Lysko K., Schwartz A. T., Taverna R. D. (1977):
- 569 *Calorimetric studies of the structural transitions of the human erythrocyte membrane. The*
- 570 *involvement of spectrin in the A transition. Biochemistry.16, 3450-3454*
- 571 Cabantchik Z. I., Greger R. (1992): Chemical probes for anion transporters of
- 572 *mammalian cell membranes. Am. J. Physiol. 262, 803-827*
- 573 Chien S. (1987): Red-cell deformability and its relevance to blood-flow. *Annu. Rev.*
- 574 *Physiol. 49, 177-192*
- 575 Ciana A., Achilli C., Balduini C., Minetti G. (2011): On the association of lipid rafts to
- 576 *the spectrin skeleton in human erythrocytes. Biochim. Biophys. Acta. 1808, 183-190*
- 577 Ciana A., Balduini C., Minetti G. (2005): Detergent-resistant membranes in human
- 578 *erythrocytes and their connection to the membrane-skeleton. J. Biosci. 30, 317-28*

579 Delicou S., Xydaki A., Kontaxi C., Maragkos K. (2015): Disorders of the erythrocyte
580 membrane. *Ital. J. Med.* 9, 323-329

581 Dodge J. T., Mitchell C., Hanahan D. J. (1963): The preparation and chemical
582 characteristics of hemoglobin-free ghosts of erythrocytes. *Arch. Biochem. Biophys.* 100, 119-
583 130

584 Fischer T. M., Haest C. W. M., Stoehr M., Kamp D., Deuticke B. (1978): Selective
585 alterations of erythrocyte deformability by SH reagents. Evidence for an involvement of
586 spectrin in membrane shear elasticity, *Biochim. Biophys. Acta.* 510, 270-282

587 Gimsa, J. Ried C. (1995): Do band 3 protein conformational changes mediate shape
588 changes of human erythrocytes. *Mol. Membr. Biol.* 12, 247-254

589 Hendrich A. B., Michalak K., Bobrowska M., Kozubek A. (1991): Effect Of Spectrin
590 On Structure Properties Of Lipid Bilayers Formed From Mixtures Of Phospholipids.
591 Fluorescence And Microcalorimetric Studies. *Gen. Physiol. Biophys.* 10, 333-342

592 Hianik T., Rybár P., Bernhardt I. (2000): Adiabatic compressibility of red blood cell
593 membrane: influence of skeleton. *Bioelectrochemistry.* 52, 197-201

594 Iglič A. (1997): A possible mechanism determining the stability of spiculated red
595 blood cells. *J. Biomech.* 30, 35-40

596 Ivanov I. T. (2001): Rapid method for comparing the cytotoxicity of organic solvents
597 and ability to destabilize proteins of erythrocyte membrane. *Pharmazie.* 56, 808-809

598 Ivanov I. T. (2010): Impedance spectroscopy of human erythrocyte membrane: Effect
599 of frequency at the spectrin denaturation transition temperature. *Bioelectrochemistry.* 78, 181-
600 185

601 Ivanov I. T., Brähler M., Georgieva R., Bäumlner H. (2007): Role of membrane
602 proteins in thermal damage and necrosis of red blood cells. *Thermochim. Acta.* 456, 7-12

603 Ivanov I. T., Paarvanova B. (2016): Dielectric relaxations on erythrocyte membrane as
604 revealed by spectrin denaturation. *Bioelectrochemistry*. 110, 59-68

605 Ivanov I. T., Paarvanova B. (2016): Dielectric relaxations on erythrocyte membrane as
606 revealed by spectrin denaturation. *Bioelectrochemistry*. 110, 59-68

607 Ivanov I. T., Paarvanova B., Slavov T. (2012): Dipole relaxation in erythrocyte
608 membrane: involvement of spectrin skeleton. *Bioelectrochemistry*. 88, 148-155

609 Jennings M. L., Passow H. (1979): Anion transport across the erythrocyte membrane,
610 in situ proteolysis of band 3 protein, and cross-linking of proteolytic fragments by 4,4'-
611 diisothiocyano dihydrostilbene-2,2'-disulfonate. *Biochim. Biophys. Acta*. 554, 498-519

612 Kell D. B. (1987): The principles and potential of electrical admittance spectroscopy:
613 an introduction, In: *Biosensors: fundamentals and applications*, (Eds. A.P.F. Turner, I.
614 Karube, G. S. Wilson), pp. 427-468, Oxford University Press, Oxford

615 Klösgen B., Rümenapp C., Gleich B. (2011): Bioimpedance Spectroscopy. In:
616 *BetaSys: Systems Biology Of Regulated Exocytosis In Pancreatic β -Cells*, Vol. 2 *Systems*
617 *Biology*. (Eds. B. Boß-Bavnbek, B. Klösgen, J. Larsen, F. Pociot, E. Renström), pp. 241-
618 271, Springer Publishing Company

619 Kralj-Iglič V., Svetina S., Žekž B. (1996): Shapes of bilayer vesicles with membrane
620 embedded molecules. *Eur. Biophys. J.* 24, 311-321

621 Low P. S., Willardson B. M., Narla M., Rossi M., Shohet S. (1991): Contribution Of
622 The Band 3-Ankyrin Interaction To Erythrocyte Membrane Mechanical Stability. *Blood*. 77,
623 1581-1586

624 Lux S. E., John K. M., Karnovsky M. J. (1976): Irreversible Deformation Of The
625 Spectrin-Actin Lattice In Irreversibly Sickled Cells. *J. Clin. Invest.* 58, 955-963

626 Mangeat P. H. (1988): Interaction of biological membranes with the cytoskeletal
627 framework of living cells. *Biol. Cell*. 64, 261-281

628 McMillan P. N., Luftig R. B. (1973): Preservation Of Erythrocyte Ghost Ultrastructure
629 Achieved By Various Fixatives. *Proc. Nat. Acad. Sci. USA.* 70, 3060-3064

630 Michalak K., Bobrowska M., Bialkowska K., Szopa J., Sikorski A. F. (1994):
631 Interaction of Erythrocyte Spectrin with Some Nonbilayer Phospholipids. *Gen. Physiol.*
632 *Biophys.* 13, 57-62

633 Mohandas N., Gallagher P. G. (2008): Red cell membrane: past, present, and future.
634 *Blood.* 112, 3939-3948

635 Mokken F. C., Kedaria M., Henny C. P., Hardeman M. R., Gelb A.W. (1992): The
636 clinical importance of erythrocyte deformability, a hemorheological parameter. *Ann.*
637 *Hematol.* 64, 113-122

638 Mukhopadhyay R., Gerald Lim H. W., Wortis M. (2002): Echinocyte Shapes:
639 Bending, Stretching, And Shear Determine Spicule Shape And Spacing. *Biophys. J.* 82, 1756-
640 1772

641 Paarvanova B., Tacheva B., Dospatliev L., Karabaliev M., Ivanov I. (2012): Polarity
642 index: a measure for the destabilization effect of organic solutes on erythrocyte membrane
643 proteins. *Trakia J. Sci.* 10, 150-154

644 Poklar N., Petrovčić N., Oblak M., Vesnaver G. (1999): Thermodynamic stability of
645 ribonuclease A in alkylurea solutions and preferential solvation changes accompanying its
646 thermal denaturation: A calorimetric and spectroscopic study. *Prot. Sci.* 8, 832-840

647 Reithmeier R. A. F., Chan S. L., Popov M. (1996): Structure Of The Erythrocyte Band
648 3 Anion Exchanger. In: *Handbook Of Biological Physics. Volume 2. Transport Processes In*
649 *Eukaryotic And Prokaryotic Organisms* (Eds. W. N. Konings, H. R. Kaback, J. S. Lolkema),
650 pp. 281-309, Elsevier Science B. V

651 Sharma S., Gokhale S. M. (2011): Solubility Behaviour Of Integral Proteins And
652 Glycophorins Of Mammalian Erythrocyte Membrane. *Asian J. Exp. Biol. Sci.* 2, 449-454

653 Shelby J. P., White J., Ganesan K., Rathod P.K., Chiu D.T. (2003): A microfluidic
654 model for single-cell capillary obstruction by *Plasmodium falciparum* infected erythrocytes.
655 *Proc. Natl. Acad. Sci. (U.S.A.)* 100, 14618-14622

656 Simchon S., Jan K. M., Chien S. (1987): Influence of reduced red-cell deformability
657 on regional bloodflow. *Am. J. Physiol.* 253, 898-903

658 Snow J. W., Brandts J. F., Low P. S. (1978): The effects of anion transport inhibitors
659 on the structural transitions in erythrocyte membranes. *Biochim Biophys Acta.* 512, 579-591

660 Tanner M. J. (1993): Molecular and cellular biology of the erythrocyte anion
661 exchanger (AE1). *Semin Hematol.* 30, 34-57

662 Van Dort H. M., Moriyama R., Low P. S. (1998): Effect of Band 3 Subunit
663 Equilibrium on the Kinetics and Affinity of Ankyrin Binding to Erythrocyte Membrane
664 Vesicles. *J. Biol. Chem.* 273, 14819-14826

665 Waugh R. E., Agre P. (1988): Reductions of erythrocyte membrane viscoelastic
666 coefficients reflect spectrin deficiencies in hereditary spherocytosis. *J. Clin. Invest.* 81, 133-
667 141

668 Wildenauer D. B., Reuther H., Remien J. (1980): Reactions of the alkylating agent
669 tris(2-chloroethyl)-amine with the erythrocyte membrane. Effects on shape changes of human
670 erythrocytes and ghosts. *Biochim. Biophys. Acta.* 603, 101-116

671 Woelders H., Malva A. P. (1998): How important is the cooling rate in
672 cryopreservation of (bull) semen, and what is its relation to thawing rate and glycerol
673 concentration? *Reprod. Dom. Anim.* 33, 299-305

674 Yu J., Fischman D. A., Steck T. L. (1973): Selective solubilization of proteins and
675 phospholipids from red blood cell membranes by nonionic detergents. *J. Supramol. Struct.* 1,
676 233-248

- 677 Zwaal R. F. A., Schroit A. J. (1997): Pathophysiologic Implications of Membrane
678 Phospholipid Asymmetry in Blood Cells. *Blood*. 89, 1121-1132

Fig. 1 [Download full resolution image](#)

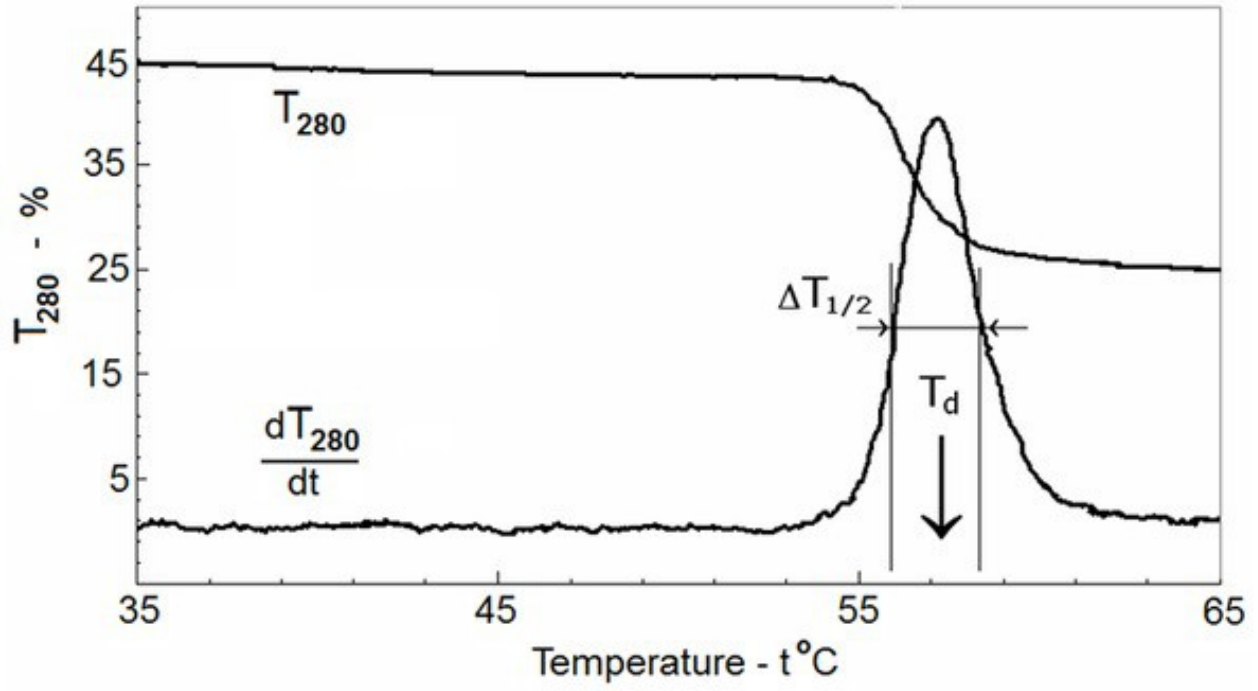


Fig. 3 [Download full resolution image](#)

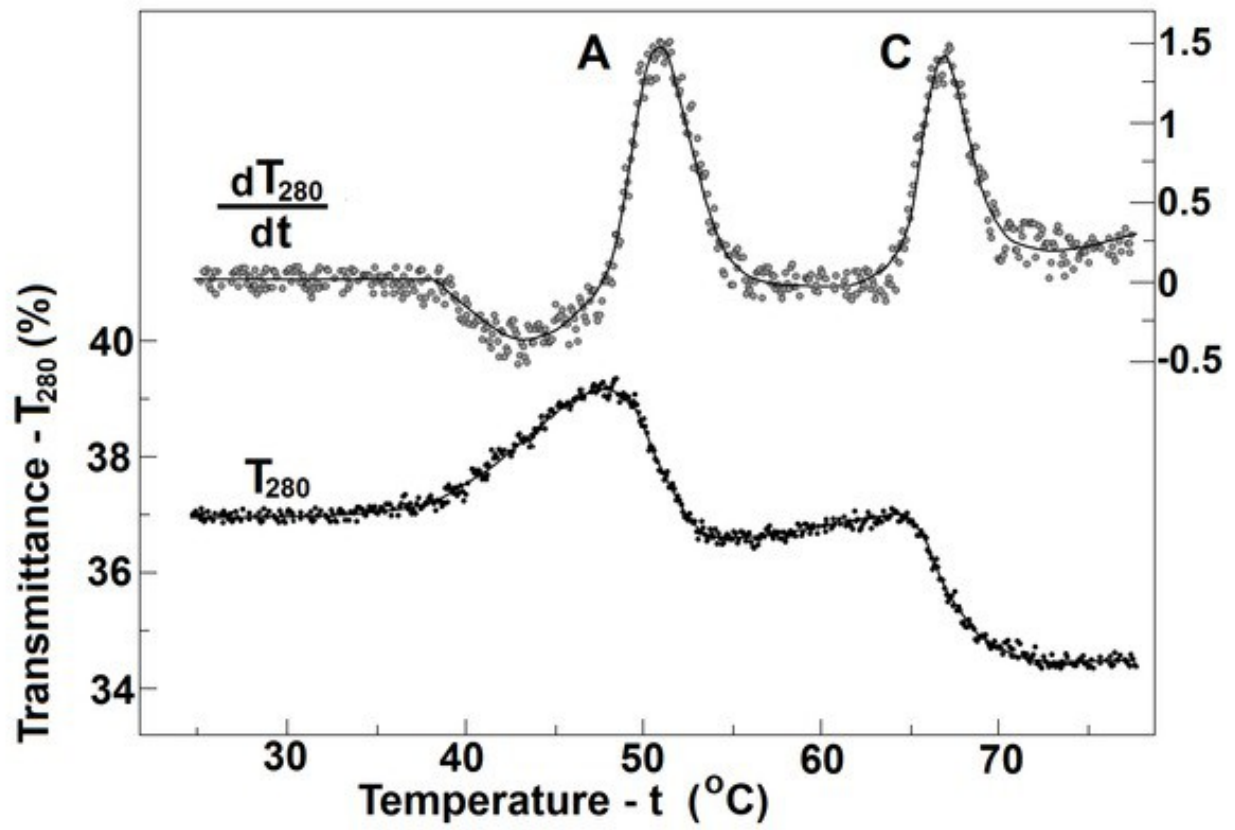


Fig. 4 [Download full resolution image](#)

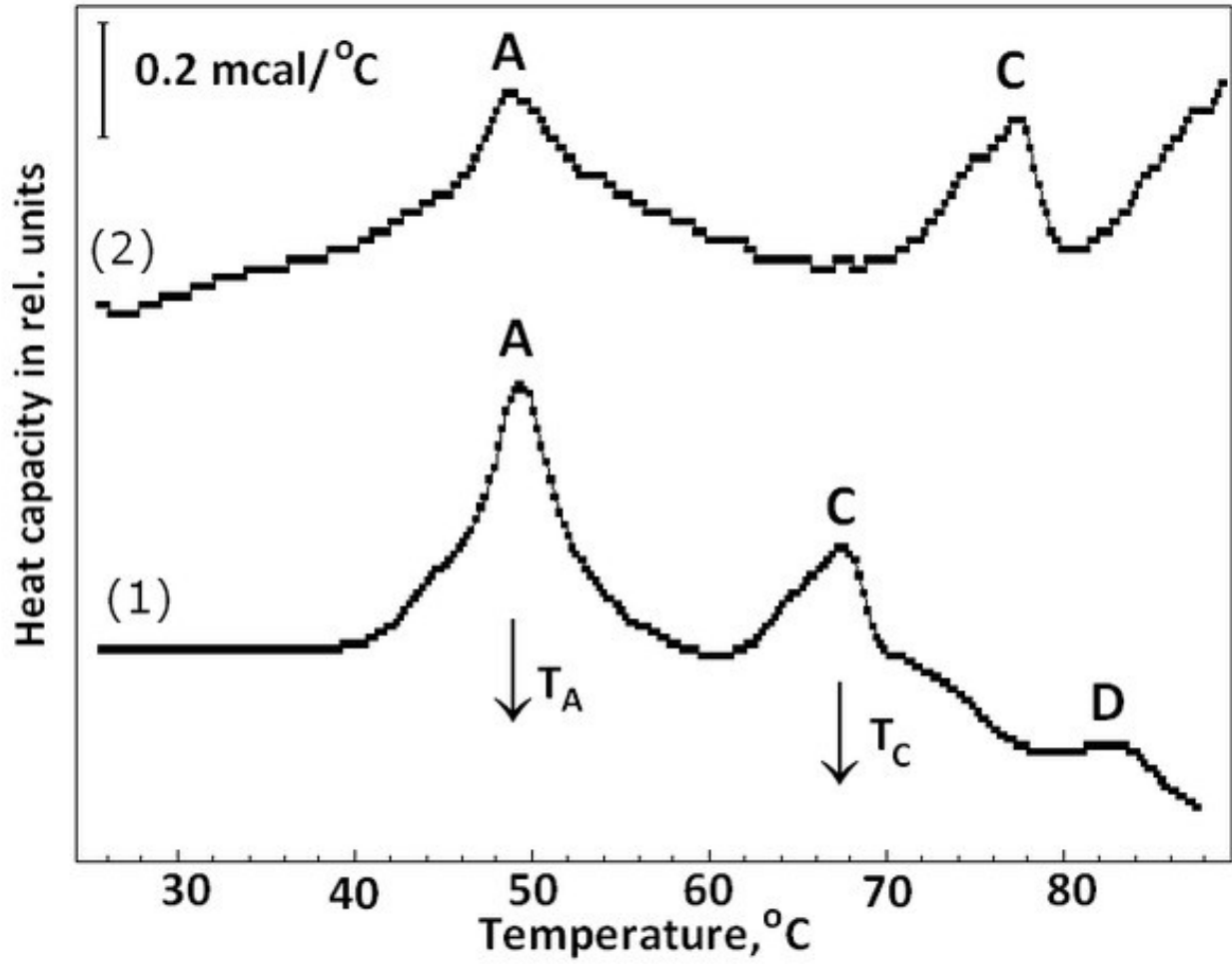


Fig. 5 [Download full resolution image](#)

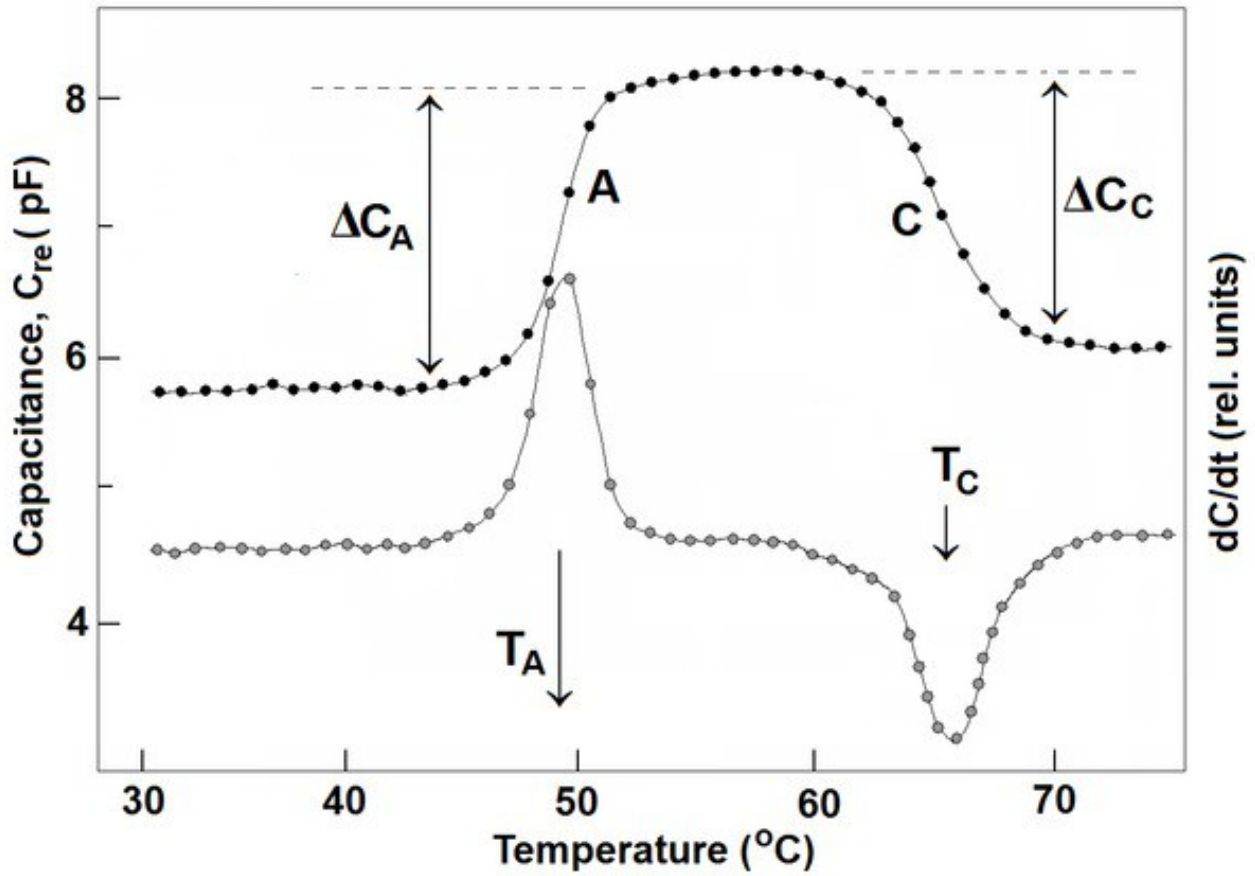


Fig. 6 [Download full resolution image](#)

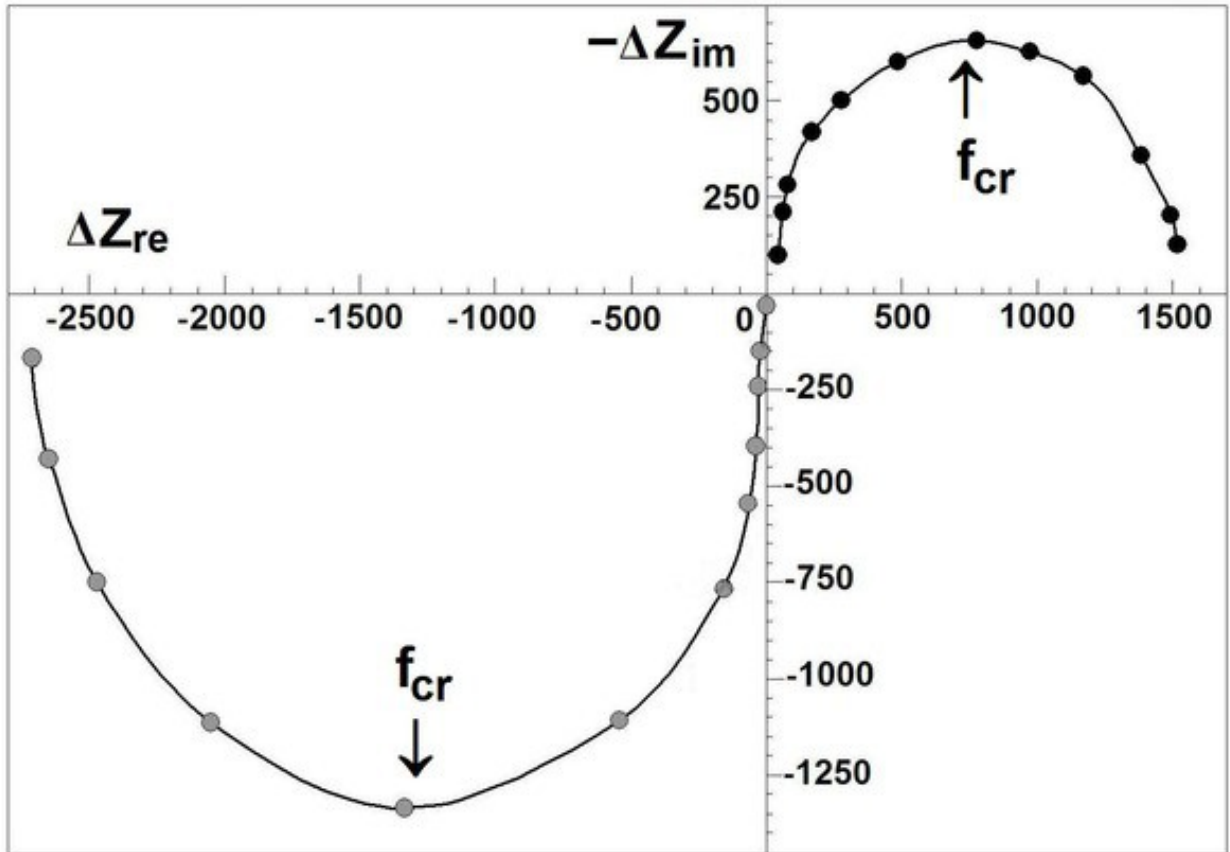


Fig. 7 [Download full resolution image](#)

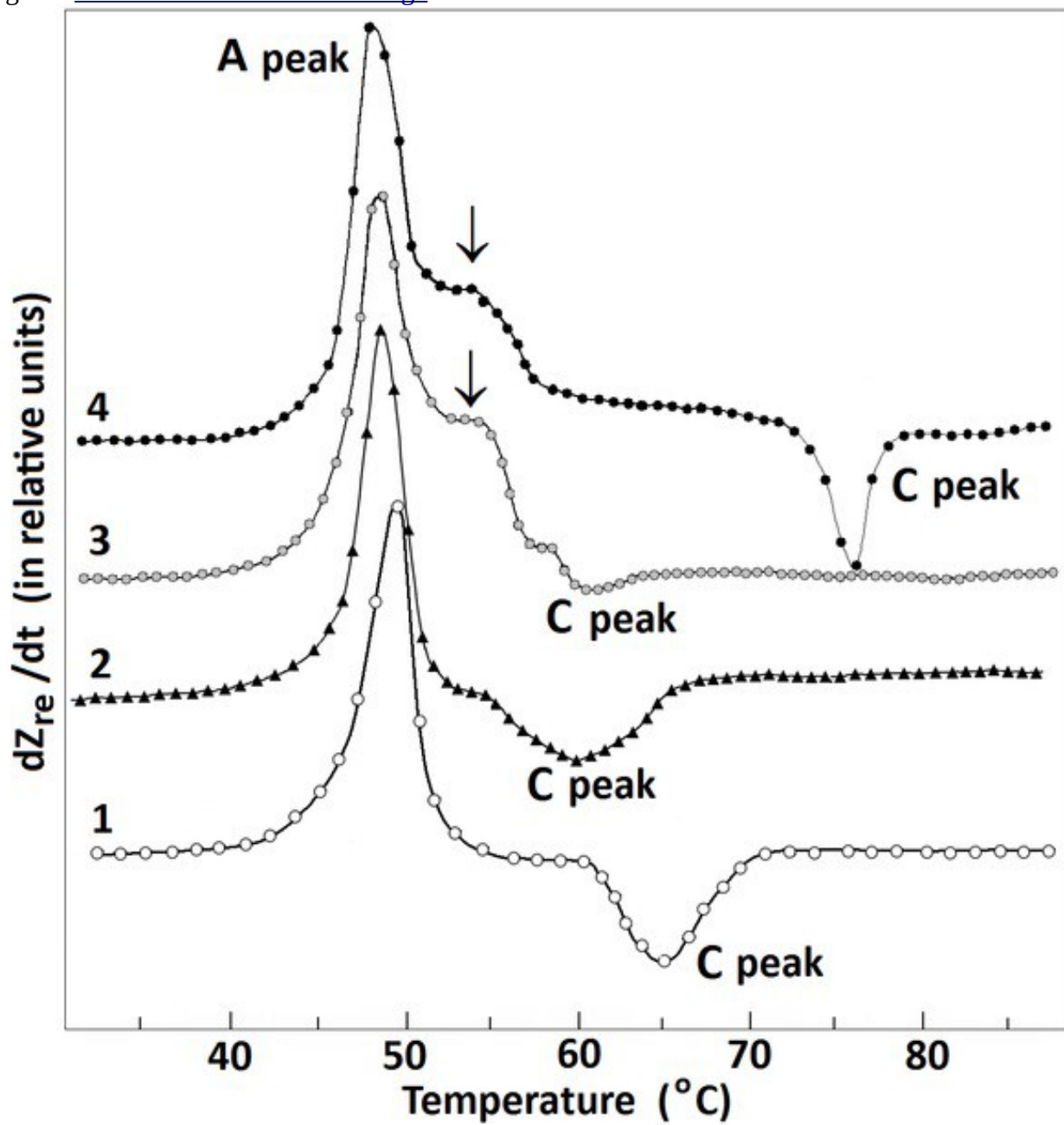


Fig. 2 [Download full resolution image](#)

